Soft Matter

PAPER

View Article Online
View Journal

Cite this: DOI: 10.1039/c6sm02102f

Wrinkling of milk skin is mediated by evaporation

Arthur A. Evans,*[a] Elliott Cheung,[b] Kendra D. Nyberg[bc] and Amy C. Rowat*[bc]

Wrinkling of thin films and membranes can occur due to various mechanisms such as growth and/or mismatch between the mechanical properties of the film and substrate. However, the physical origins of dynamic wrinkling in soft membranes are still not fully understood. Here we use milk skin as a tractable experimental system to investigate the physics of wrinkle formation in a thin, poroelastic film. Upon heating milk, a micron-thick hydrogel of denatured proteins and fat globules forms at the air–water interface. Over time, we observe an increase in the total length of wrinkles. By confocal imaging and profilometry, we determine that the composition and thickness of the milk skin appears to be homogeneous over the length scale of the wrinkles, excluding differences in milk skin composition as a major contributor to wrinkling. To explain the physical origins of wrinkle growth, we describe theory that considers the milk skin as a thin, poroelastic film where pressure is generated by the evaporative-driven flow of solvent across the film; this imparts in-plane stresses in the milk skin, which cause wrinkling. Viscous effects can explain the time-dependent growth of wrinkles. Our theoretical predictions of the effects of relative humidity on the total length of wrinkles over time are consistent with our experimental results. Our findings provide insight into the physics of the common phenomenon of milk skin wrinkling, and identify hydration gradients as another physical mechanism that can drive morphological instabilities in soft matter.

Received 15th September 2016,
Accepted 12th December 2016

DOI: 10.1039/c6sm02102f

www.rsc.org/softmatter

1 Introduction

Wrinkling in soft matter systems is ubiquitous from the undulated surfaces of peas and soy bean skin to cell nuclei and bacterial biofilms (Fig. 1). Such wrinkling transitions can be driven by various mechanisms.[1] Competition between two or more material properties, such as in the case of films floating on liquids,[2] gives rise to a length scale over which elastic stress due to pressure or residual stress may be alleviated through wrinkling. When the film is attached to a solid substrate, such as in solid core–shell systems as a drying pea[3] or a cell nucleus with a soft gel interior,[4] wrinkling of the shell can relieve in-plane stresses via bending and in-plane compression, but requires also bulk deformation of the underlying core material; the morphology of wrinkles depends on the competition between these two mechanisms.[3,5,6] Wrinkling can also be mediated by patterning the underlying surface with cracks.[7,8] Mass transport processes, such as growth, can additionally drive wrinkled morphologies. For instance, the characteristic wrinkling of biofilms at air–water interfaces (pellicles) can be described by residual stresses that are induced during growth.[9] Similarly, a change in volume due to swelling or dessication can result in wrinkling.[3,10–12] The prevalence of wrinkling induced by dehydration on both solid and liquid substrates, from fruits and vegetables[3,13,14] to hydrogels,[12] suggests a common link between mass transport and residual stress in thin materials of many disparate types.

Milk provides an intriguing system for examining how mass transport can drive morphological change: upon heating a pot of liquid milk, a milk 'skin' forms within minutes as proteins in solution denature and are driven to the air–liquid interface where they aggregate to form a thin, poroelastic film (Fig. 2). Such milk skins have various culinary applications, from the dairy milk skins of sweet Indian delicacies to the use of soy milk skins or 'yuba' in Japanese cuisine. Of interest from a physics perspective, milk skins typically exhibit wrinkling. The denaturation temperatures of the main whey and casein protein components of milk are well-characterized[15] due to the implications of thermally-induced aggregation in milk processing and packaging. The molecular composition of the resultant aggregates in bulk milk,[15,16] and at air–liquid interfaces[17,18] are also well-studied. However, the physical origins of wrinkling in milk skins are not fully understood. For example, the extent to which spatial segregation of chemical components in the milk skin, such as proteins and lipids, contribute to wrinkles or other morphological deformations remains to be determined.[19] Evaporation of solvent that is enhanced by heating could also induce stresses that lead to wrinkling.

[a] Department of Mathematics, University of Wisconsin, Madison, Madison, USA
[b] Department of Integrative Biology and Physiology, University of California Los Angeles, Terasaki Life Sciences Building, 610 Charles E Young Drive South, Los Angeles, USA
[c] Department of Bioengineering, University of California Los Angeles, Los Angeles, USA. E-mail: rowat@ucla.edu; Tel: +1 310 825 4026

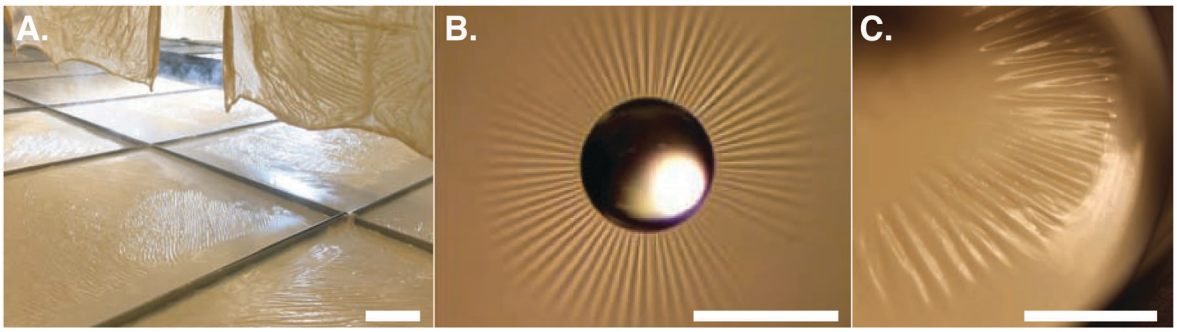

Fig. 1 Examples of wrinkles in thin films and skins. (A) Soy milk skin. Scale, 10 cm. Image courtesy Hodo Soy. (B) Droplet on a thin polymer film.[6] Scale, 1 mm. From Huang *et al.* (2007) Science. Reprinted with permission from AAAS. (C) Milk skin with positive air pressure applied to the center of the film. Scale, 5 cm.

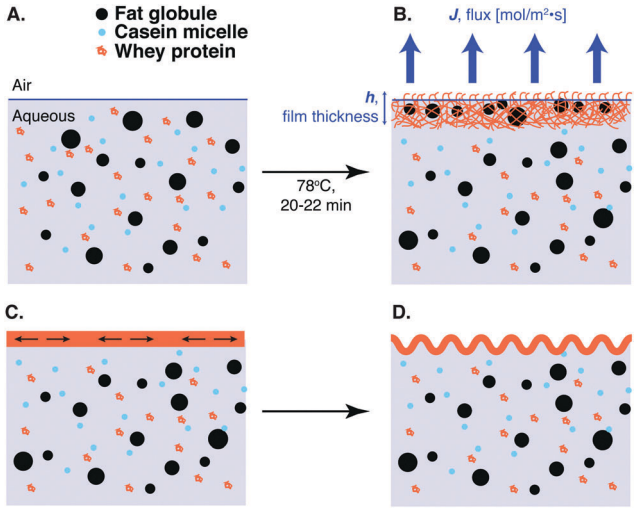

Fig. 2 Schematic illustrations showing (A) the components of liquid milk; (B) the structural changes that occur upon heating; and (C) our proposed physical model of how flow of solvent across the milk skin can result in mechanical stresses (black arrows) that drive wrinkling, as shown in (D). Drawings are not to scale.

Here we investigate the physics of wrinkling in milk skin, which we consider as a poroelastic membrane that exhibits an increasing length of wrinkles over time. To examine heterogeneities in milk skin composition as a possible source of wrinkles, we measure milk skin thickness using profilometry and determine the spatial composition on the micron-scale using confocal microscopy. We then examine how evaporation influences the wrinkling, by observing wrinkle growth by time-lapse imaging of milk skins that are maintained in a humidity-controlled chamber (Fig. 3). Our results reveal that the rate of wrinkle growth depends on the relative humidity and can be described using theory to describe the evaporation-dependent stresses in a thin, poroelastic film. Taken together our findings provide insight into the physical origins of the common, everyday phenomenon of milk skin wrinkling and illustrate how the wrinkling of thin films can be controlled by a hydration gradient.

2 Experimental methods

Milk skin formation

Whole milk is purchased from a local grocery store. To enhance contrast during imaging, we add 4 drops of 1% v/v blue food coloring (Kroger) to 200 mL of milk. The dyed milk is heated in a 125 mm diameter pyrex dish on a hot plate to a temperature of 78 °C over 20 to 22 minutes. We record the temperature in

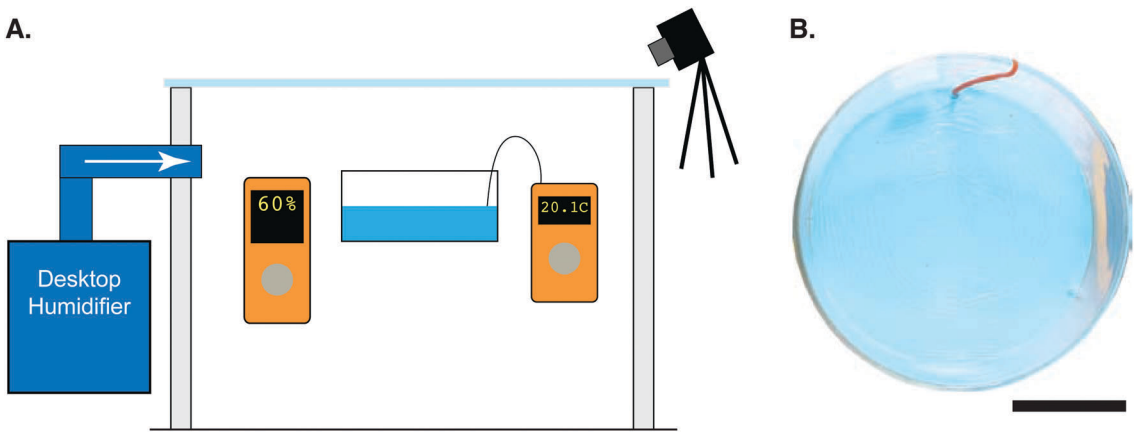

Fig. 3 Observing milk skins. (A) Schematic illustration of the humidity-controlled imaging chamber used to observe wrinkle formation in milk skin. (B) Image shows a milk skin that has formed after the cooling period at 60% RH. Scale, 5 cm.

the milk using a thermocouple (Fluke). Once the film has formed, which occurs after approximately 20 to 22 minutes of heating, the dish is removed from the heat and placed in a home-built imaging chamber, which consists of a styrofoam box outfitted with a digital camera (Nikon DXX00 Digital SLR, Nikon) (Fig. 3A). We begin to image milk skins after an 11 minute cooling period either in ambient humidity (for 30 or 60% RH films) or 90% RH for high humidity films. Humidity in the imaging chamber is regulated using a desktop humidifier (Sunpentown International Inc.) and monitored using a humidistat (Reed).

Imaging wrinkle growth in milk skins

To reproducibly investigate the dynamics of wrinkle formation, we induce axisymmetric nucleation of wrinkles by placing a well-defined mass in the center of the milk skin. We mold a 1.75 mm × 3.5 mm polymer disc (0.114 g) by filling a drinking straw (diameter, 1.75 mm) with polydimethylsiloxane (PDMS) with 1 : 10 crosslinker (Sylgard 184 Silicone Elastomer, Dow Corning) and curing at 65 °C for 1 hour; we then slice a cylinder with a height of approximately 3.5 mm. We place the mass in the center of the dish at the end of the cooling period and acquire images at 5 minute intervals. Subsequent image analysis is performed using ImageJ (National Institutes of Health). We evaluate the total length of all wrinkles that originate from the polymer mass and track this length over time. We include the length of wrinkles that branch off from parent wrinkles, where their origin is the branching point from the parental wrinkle. Only wrinkles that directly connect to the parental wrinkle are included in our wrinkle length analysis.

Imaging micron-scale structure of milk skins

To visualize the spatial distribution of fat globules in milk skins, we stain milk prior to heating with the lipophilic, Nile red dye (Sigma-Aldrich), and image the resultant milk skin by confocal microscopy. Nile red is prepared in ethanol at 1 g mL^{-1} stock solution and used at a final concentration of 2.0% v/v. Milk is heated to 78 °C and the resultant milk skin is placed at ambient temperature and humidity to develop for the cooling period. Nile red has no observable effects on milk skin formation or wrinkle growth. To extract the milk skin for imaging, we cut a slit in the milk skin using a razor blade and insert a 10 cm diameter silicon wafer below the film. The milk skin is mounted on top of the wafer by slowly lifting the wafer out of the dish at a 45° angle. We image milk skins using a confocal microscope (Zeiss LSM 5 Exciter, Zeiss) equipped with a 63×/N.A. 1.2 objective and 488 nm argon laser for excitation. We also image fat globules in liquid milk by placing a small amount of Nile-red stained milk between glass coverslips.

Milk skin thickness

To determine how the thickness of the milk skin changes during wrinkle development, we isolate the milk skin for thickness measurements following the same procedure, using a razor blade to extract a small piece of milk skin, and mounting it onto a 10 cm diameter silicon wafer. We measure the thickness of isolated milk skins using a surface profilometer (Dektak 150, Veeco). To sample a larger area of milk skin without direct contact, we use refractive profilometry (Nanospec AFT 2100, Nanometrics), calibrating using our thickness measured by surface profilometry. For each time point, 10 thickness measurements are obtained across the area of the skin.

3 Results

3.1 Milk: from liquid to film

Milk is a complex dispersion of fat globules and casein micelles in an aqueous suspension of whey proteins, soluble caseins, salts, and lactose. The thermodynamic properties of milk and milk proteins are well-studied. Denaturation of the major whey proteins in milk, including beta-lactoglobulin and alpha-lactalbumin, occurs between 62–78 °C.[15,20,21] Thus, we heat our sample to 78 °C where predominantly whey proteins denature; at higher temperatures, casein proteins also denature.

Protein denaturation is followed by subsequent aggregation.[15,16] The aggregation of denatured milk skin proteins is a spontaneous thermodynamic process and can be attributed to bonding through hydrogen bonds or disulfide bridges that form between thiol groups of cysteine residues,[15,16,22] as well as hydrophobic interactions that occur when hydrophobic regions of the proteins, which are otherwise buried for proteins under ambient conditions in solution, become exposed upon heating. Hydrophobic interactions are a main driving force for self-assembly, as protein aggregation can minimize contacts of the hydrophobic regions with water.[15,23] Driving forces for self-assembly can also involve intermolecular interactions as well as entropic contributions resulting from release of counterions and water molecules[24,25] and entropic gain due to increased conformational freedom of unfolded amino acid chains.[16,26] In the formation of a 2D milk skin, there is also entropic gain originating from the release of water molecules caging proteins in bulk phase and subsequent rearrangement of protein structure upon adsorption to air–water interface. The overall result is a porous meshwork of proteins and fat globules at the air–liquid interface (Fig. 2).

Upon heating the milk to 78 °C, we observe that a solid patch forms on the surface of the milk near the center of the dish; the patch then spreads to the walls of the dish, consistent with a nucleation and growth process. Once the film touches the edges of the dish, wrinkles begin to form near the edges of the dish; this may reflect the stresses that arise due to contact with the walls. After 20 to 22 minutes at 78 °C, a continuous, thin, film can be observed at the air–milk interface (Fig. 3B). The resultant milk skin exhibits solid characteristics: it can be lifted off the liquid milk substrate and is subject to folding and tearing. The film can also exhibit wrinkles, which are accentuated by applying an external stress to the milk skin, for example by blowing across the skin or applying a gentle positive pressure on the center of the skin (Fig. 1C).

3.2 Milk skin has a homogeneous composition on the length scales of wrinkles

One possible origin of the wrinkled morphology of the milk skin is underlying heterogeneity in its composition on the length

scale of the wrinkles. Since milk consists of both fat globules and proteins in an aqueous solution, phase separation of these components in the solidified milk skin could result in spatial heterogeneity of the milk skin mechanical properties, with some regions where bending and deformation is more energetically favorable. A propensity for out-of-plane deformations by domains in other solid-elastic membranes, such as the lamina network of the nuclear envelope, can explain the formation of blebs in the cell nucleus.[19] Therefore we next sought to determine if the wrinkles correspond to heterogeneity in the lateral organization of the milk skin.

To address the potential contributions of heterogeneities on the 10^{-3} m length scale of wrinkles in the milk skin, we fluorescently label the fat globules and image the milk skin by confocal microscopy. We first examine the micron-scale structure of liquid milk that is stained with the lipophilic dye, Nile red. The fat globules have a mean diameter of 1.35+/−0.08 μm in diameter and thus exhibit Brownian motion in the liquid milk. In contrast to the liquid milk, fat globules in the milk skin are stationary with respect to each other, suggesting they are entrapped in the network of proteins that forms upon denaturation. Imaging the spatial distribution of fat globules in milk skin reveals that they are evenly distributed (Fig. 4A). Thus, on the 10^{-3} m length scale of the wrinkles, the milk skin has a homogeneous composition, which thus cannot explain the origins of wrinkling.

Another possible contribution to wrinkle formation could be variations in the thickness of the film; the bending modulus of a planar membrane depends on thickness as $\kappa \sim d^3$ and the film thickness can determine the wavelength of wrinkles.[13] To investigate milk skin thickness, we use surface and refractive profilometry to measure the thickness of the milk skin at varying positions across the skin. Our results reveal that milk skin thickness increases with time after the initial film formation to a plateau of around 34.5 to 35.0 μm (Fig. 4B), which corresponds to the time when our imaging of wrinkle growth begins. The error that we observe between experiments is within our measurement error, thus we observe no significant differences in milk film thickness as wrinkles elongate and develop over time.

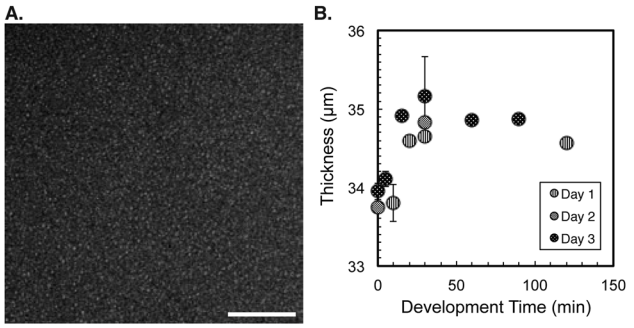

Fig. 4 Milk skin composition is homogeneous on the length scale of wrinkles. (A) Confocal image of milk skin labeled with Nile red to visualize fat globules. Scale, 20 μm. (B) Milk skin thickness as a function of aging time determined by refractive profilometry. Each data point represents 10 thickness measurements acquired across a 8 × 8 cm^2 area of milk skin for 2 independent experiments. Error bars represent standard deviation.

Asymmetry in composition across a membrane can contribute to spontaneous curvature and out-of-plane bending.[27–29] Due to the hydration gradient across the milk skin, there could be asymmetry in the mechanical properties of the film. For example, at low relative humidity, the air interface may be less hydrated, and therefore have a slight difference in polymer density, which could alter the bending modulus relative to the liquid interface. Variation in molecular composition through the depth of skin could result from preferential movement of smaller components through the hydrogel, which have faster diffusion coefficients than larger protein components of milk.[18] Creaming of fat may also occur.[18] While we cannot exclude that compositional asymmetry may contribute to out-of-plane bending, the expected radius of curvature of any resultant bending would be on the length scale of the skin thickness, around 10^{-5} m. By contrast, the wrinkles that we observe are 10^{-4} to 10^{-3} m. Therefore we do not expect that the wrinkling that we observe is driven by compositional asymmetry of the milk skin.

3.3 Wrinkling of milk skins

Another possible origin of morphological transitions in thin film and membrane systems is dehydration. We observe that the wrinkles appear as the milk skin ages. Wrinkles can be more reproducibly induced by applying external stresses on the film; for example, by blowing gently across its surface.

To generate a tractable experimental system that enables us to systematically measure wrinkle length, we exert a controlled external stress on the film by placing a well-defined small, 1.75 mm × 3.5 mm, cylindrical mass of silicone polymer (PDMS) on the center of the milk skin after it has cooled. The mass reproducibly exerts well-defined radial stresses on the milk skin and thus enables us to determine how the length of wrinkles evolves with time. We also observe the formation of patches of wrinkles that have random orientations and varying distances from the edges of the dish. However, due to the variable boundary conditions of such peripheral wrinkles, we exclude these from our analysis and instead focus on the wrinkles that radiate out from the central mass.

Under ambient conditions, we observe that wrinkles consistently radiate out from the mass, where maximal tension is generated in the film. Over 0 to 50 min, the total wrinkle length increases (Fig. 5). The wrinkle length then plateaus, as wrinkles contact the edges of the petri dish and/or the boundary layer of peripheral wrinkles around the perimeter of the dish.

3.4 Milk skin as a poroelastic thin film

To test our hypothesis that dehydration contributes to the wrinkling of milk skins, we describe a theory that considers the milk skin as a thin poroelastic film of thickness h, resting on a liquid substrate whose evaporation acts as the primary source of in-plane stresses[30–32] (Fig. 2B and C).

Once formed, the milk skin contains a mixture of solvent with concentration c, which evaporates from the film through a flux J (Fig. 2).

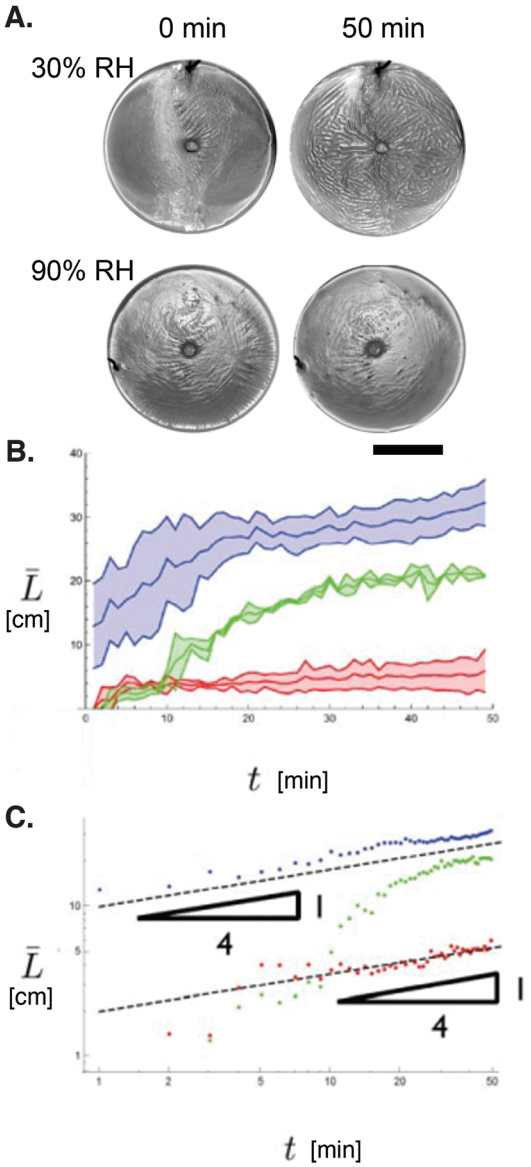

Fig. 5 Wrinkle formation in milk skins depends on time and relative humidity (RH). (A) Representative images of milk skin at 30% and 90% RH at 0 and 50 min. Scale, 6 cm. (B) Average total wrinkle length as a function of time. Blue: 30% RH; green: 60% RH; and red 90% RH. Line shows the average wrinkle length from at least $N = 2$ independent experiments. Shaded area represents standard deviation. (C) Average total wrinkle length on a log–log scale shows the power-law dependence.

For such a poroelastic film, mechanical equilibrium and conservation of mass demand that

$$\partial_t c + \nabla\cdot\mathbf{J} = 0, \tag{1}$$

$$\nabla\cdot\boldsymbol{\sigma} = 0, \tag{2}$$

where $\boldsymbol{\sigma}$ is the poroelastic stress tensor. Closing this system requires constitutive relations for the stress and the concentration:

$$\sigma_{ij} = \frac{Y}{1+\nu}\left[\frac{\nu}{1-2\nu}\delta_{ij}\varepsilon_{kk} + \varepsilon_{ij}\right] - p\delta_{ij}, \tag{3}$$

where Y is the Young's modulus and ν is Poisson's ratio. Here the usual stress tensor for Hookean elasticity is supplemented by the pore pressure p, which is related to the evaporative flux through Darcy's law:

$$\mathbf{J} = -\frac{k}{\eta}\nabla p, \tag{4}$$

where k is the permeability of the gel and η is the dynamic viscosity of the solvent. The gel is assumed to be elastically incompressible. If we assume that we have a thin film with a constant evaporation rate J (in units of mol per area per time), the thin film approximation allows us to use a thickness-averaged pore pressure $\langle p\rangle \sim Jh\eta/k$.

3.5 Dynamics of wrinkle growth

In addition to the static equilibrium conditions for wrinkling of hydrogels, or the steady state effects of evaporation-induced stresses, there may be viscous stresses that dissipate over time and lead to the dynamic evolution of patterns.[33] We start with a simple one-dimensional model for wrinkling of a thin film, given by the following equations for in-plane and normal stress balance:

$$\partial_x\sigma = T, \tag{5}$$

$$\xi\frac{\partial\zeta}{\partial t} + B\partial_x{}^4\zeta - h\sigma\partial_x{}^2\zeta - T\partial_x\zeta = \rho g\zeta. \tag{6}$$

Here we have the normal displacement ζ, the bending modulus B of the skin, a damping coefficient ξ, an applied tension T, and a hydrostatic pressure from the substrate that is given by ρg. Assuming $T = 0$, this predicts that there is a constant elastic stress in the film.

Hooke's law for an isotropic solid then relates the elastic stress to the strain:

$$\sigma = \sigma^s + \frac{Y}{1-\nu^2}\varepsilon, \tag{7}$$

where σ^s is the stress induced by shrinkage of the film and the nonlinear strain is given by:

$$\varepsilon = \partial_x u + \frac{1}{2}(\partial_x\zeta)^2, \tag{8}$$

where u is the in-plane deformation and ζ is out-of-plane deflection. In the absence of any deformation, where $u = \zeta = 0$, there will be no elastic stress such that $\sigma = 0$, and the residual stress will be provided by the pore pressure $\langle p\rangle$.

Assuming a periodic solution for the height field $\zeta = A\sin qx$, the following dispersion relation must be satisfied in steady state:

$$Bq^4 + h\sigma q^2 - \rho g = 0. \tag{9}$$

The stress σ here should be treated as an applied load, and we look for a critical value $\sigma = \sigma_c$ such that there are non-trivial solutions. This gives results for the wavenumber and critical stress as $q \sim (\rho g/B)^{1/4}$ and $\sigma_c \sim \sqrt{\rho g B}/h$.

Taken together, our theory shows that the stress in the skin is generated by pore pressure $\langle p\rangle$ due to the evaporative flux; thus with a high relative humidity, evaporation is insufficient to

drive wrinkling. For low humidity, wrinkles spontaneously develop. While the linear model predicts an unstable wrinkle length scale that grows most quickly, there is a family of wrinkle wavelengths that are allowed by the dynamics. We may characterize the stress due to a particular wavelength $\lambda_q = 2\pi/q$ as $\sigma_q \sim -B/(h)q^2$. This stress may be relieved by changing the wavelength, which occurs over a timescale $\tau_q \sim B/(h\sigma_q)^2$, and which yields a scaling law for wavelength coarsening of $\lambda \sim (Bt)^{1/4}$.

3.6 Milk skin wrinkling depends on humidity

To test the prediction from our theory that the rate of evaporation of water from the underlying liquid milk determines the wavelength of wrinkles in the milk skin, we observe the milk skins in our imaging chamber with well-controlled relative humidity (RH) ranging from 30% to 90% RH. We determine the increase in total wrinkle length, which reflects an increase in number and length of wrinkles.

With typical ambient humidities of 60% RH, we observe that some random wrinkles begin to appear already during the cooling period, even before the polymer mass is placed on the milk skin. When the mass is placed onto the center of the skin, we observe a larger number of wrinkles that radiate out from the mass. Some of the wrinkles continue to elongate until they hit edge of dish. For other wrinkles, their growth appears to be hindered by pre-existing wrinkles, which form during the cooling period. We also observe that other wrinkles grow and stop without an apparent obstacle. The average length of wrinkles increases most quickly with a growth rate of 0.8 mm minute^{-1}, and plateaus at around 30 minutes. While an increasing number of wrinkles radiate out from the mass, we also observe that wrinkles begin to branch off from the original parent wrinkles that radiate from the mass.

To test the prediction of our theory that lower RH will result in faster wrinkle growth, as well as a larger number of wrinkles that form spontaneously, we image milk skins under dry weather conditions when the ambient humidity is naturally low, around ~30% RH. At such low RH, we observe that wrinkles form within minutes after removal of the milk from the heat. These results are consistent with our prediction that a lower % RH will result in a larger hydration gradient across the film, increased in-plane stresses, and thus a larger number of wrinkles that form spontaneously even after a short time. Thus, some wrinkles are already present when the weight is placed in the center of the film at the end of the cooling period. In response to the applied stress in the center of the film, some wrinkles disappear as the film becomes taut; some reorient so they are radiating out from the mass. Under these low humidity conditions, wrinkles elongate from the mass at an initial rate of about 0.7 mm minute^{-1} over 5 to 10 minutes until they have reached the edges of the petri dish or the boundary layer of wrinkles. In addition to the wrinkles, we also observe that folds appear more frequently at this low humidity. While we observe some folding at 60% RH, there is an increased number of folds at 30% RH. These regions with deeper invaginations are typically 2 to 3 cm in diameter. Such regions with high curvature reflect additional relaxation of surface stresses and are also observed in pellicles.[9]

We next investigate if the wrinkles of a 30% RH skin can be abolished by restoring the film to a high humidity environment. We subject a skin, which is developed for 1 h at 30% RH, to a 90% RH environment for 3 hours. While some folds in the milk skin appear to become more shallow, the wrinkles do not recede over our experimental timescale. However, since the diffusion coefficients of small molecules through milk skins are observed to decrease over time,[18] water may not be able to penetrate into the milk skin on this timescale and relieve the stresses. Thus, while a planar surface cannot be completely recovered on this relatively short time scale, these results also indicate that humidity influences wrinkle morphology.

To further test the dependence of wrinkle growth on evaporation, we place milk skins in our imaging chamber with a high humidity of 90% RH. At this higher RH, we predict a lower pore pressure, and thus reduced stresses that should result in less wrinkling. Immediately following milk skin formation the surface is relatively smooth, even upon placement of the polymer mass. Over tens of minutes, wrinkles begin to radiate out from the polymer mass, but they elongate more slowly and consistently at an initial rate of approximately 0.6 mm minute^{-1}, and quickly plateau after about 6 minutes to an average length of 5.0+/−1.5 mm. Compared to the wrinkles observed in films at higher humidities, there is a reduced total wrinkle length at 90% RH, reflecting how there are fewer wrinkles that are also shorter (Fig. 5). For example, the total wrinkle length at 90% RH is approximately 20% of the total wrinkle length at 30% RH, which is on average 27+/−2 mm. We also observe that the folds at 90% RH appear to be more shallow compared to the deeper invaginations in the lower 30% RH films.

Taken together, our experimental results provide evidence that wrinkle growth strongly depends on the relative humidity of the milk skin environment, and thus rate of evaporation.

4 Discussion & conclusions

Here we show that the wrinkling of milk skins occurs due to a transverse hydration gradient that drives evaporation and induces stresses in the milk skin, which are alleviated through wrinkling. Our results provide insight into the physical origins of this common phenomenon and highlight an additional experimental parameter that can be tuned to regulate the morphology and properties of thin films, for example in polymer applications. Dehydration-induced wrinkling of other thin film systems has been investigated and accompanying theory considers the mechanical properties of the film to describe the wavelength of resultant wrinkles.[3,12] While various geometries and materials have been studied in the context of wrinkling, the time-dependent measurement of wrinkle coarsening in evaporation-driven systems has remained poorly understood. Even for a complex material as milk, which contains various types of macromolecules that denature at varying temperatures, the physical mechanism of wrinkling appears to be well-described by a simple scaling argument.

This strong agreement between theory and experiment indicates that the pore pressure induced by evaporative flow contributes

to the formation of wrinkles in the milk skin. Our theory could further be tested by investigating the wrinkling behavior of different types of milk that have distinct molecular compositions. For example, skim milk has a lower fat content; milk from other animals, such as buffalo, has higher protein content. Indeed, the resistance to evaporative diffusion is higher for skins made from milks that have higher protein, fat, and lactose contents;[18] thus by varying the type of milk, we could vary the diffusion coefficient of solvent through the milk skin, and thus vary J. Based on our results, we predict that skim milk, which has a lower fat content than whole milk, and thus potentially increased J, would exhibit more wrinkling compared to the milk skins that we study here.

Our work also provides the basis for investigating other aspects of morphological changes in thin films. Our experimental setup should enable more detailed study of the dynamics of wrinkle growth in response to a local load. While we report here on the growth of wrinkles in milk skins, we also observe larger amplitude folds that occur, which indicate the nonlinear behavior of these thin films with increasing stresses. Further studies focusing on the complex and dynamic behaviors of milk skins could deepen our knowledge of morphological instabilities in thin films.

While we demonstrate that our hypothesis can predict wrinkling of milk skins, our findings can be more broadly applied to other systems that exhibit morphological changes due to mass transport processes. Mass transport and/or growth processes may also drive morphological transitions in many other soft matter systems from biofilms to the cell nucleus during malignant transformation.

Acknowledgements

We thank Hodo Soy for sharing their image of soy milk skins in Fig. 1. We are grateful to funding from the National Science Foundation (CAREER DBI-1254185 to ACR) and the Farber Family Foundation.

References

1 B. Li, Y.-P. Cao, X.-Q. Feng and H. Gao, *Soft Matter*, 2012, **8**, 5728–5745.
2 H. Diamant and T. A. Witten, *Phys. Rev. Lett.*, 2011, **107**, 164302.
3 B. Li, F. Jia, Y.-P. Cao, X.-Q. Feng and H. Gao, *Phys. Rev. Lett.*, 2011, **106**, 234301.
4 A. C. Rowat, D. E. Jaalouk, M. Zwerger, W. L. Ung, I. A. Eydelnant, D. Olins, A. Olins, H. Herrmann, D. A. Weitz and J. Lammerding, *J. Biol. Chem.*, 2013, **288**, 8610–8618.
5 C. Fogle, A. C. Rowat, A. J. Levine and J. Rudnick, *Phys. Rev. E: Stat., Nonlinear, Soft Matter Phys.*, 2013, **88**, 052404.
6 J. Huang, M. Juszkiewicz, W. H. De Jeu, E. Cerda, T. Emrick, N. Menon and T. P. Russell, *Science*, 2007, **317**, 650–653.
7 D. Wu, Y. Yin, H. Xie, Y. Shang, C. Li, L. Wu and X. Dai, *Sci. China: Phys., Mech. Astron.*, 2014, **57**, 637–643.
8 D. Wu, Y. Yin, F. Yang and H. Xie, *Appl. Surf. Sci.*, 2014, **320**, 207–212.
9 M. Trejo, C. Douarche, V. Bailleux, C. Poulard, S. Mariot, C. Regeard and E. Raspaud, *Proc. Natl. Int. Ed.*, 2013, **110**, 2011–2016.
10 E. Hannezo, J. Prost and J.-F. Joanny, *Phys. Rev. Lett.*, 2011, **107**, 078104.
11 A. Viallat, J. Dalous and M. Abkarian, *Biophys. J.*, 2004, **86**, 2179–2187.
12 R. Rizzieri, L. Mahadevan, A. Vaziri and A. Donald, *Langmuir*, 2006, **22**, 3622–3626.
13 E. Cerda and L. Mahadevan, *Phys. Rev. Lett.*, 2003, **90**, 074302.
14 E. Cerda, *J. Biomech.*, 2005, **38**, 1598–1603.
15 H. Singh and P. Havea, *Thermal Denaturation, Aggregation and Gelation of Whey Proteins in Advanced Dairy Chemistry-1 Proteins: Part A/Part B*, Springer US, Boston, USA, 2003, vol. 90, ch. 28, pp. 1261–1287.
16 R. Mezzenga, P. Schurtenberger, A. Burbidge and M. Michel, *Nat. Mater.*, 2005, **4**, 729–740.
17 P. Atkinson, E. Dickinson, D. Horne and R. Richardson, *J. Chem. Soc., Faraday Trans.*, 1995, **91**, 2847–2854.
18 S. Kentish, M. Davidson, H. Hassan and C. Bloor, *Chem. Eng. Sci.*, 2005, **60**, 635–646.
19 C. M. Funkhouser, R. Sknepnek, T. Shimi, A. E. Goldman, R. D. Goldman and M. Olvera de la Cruz, *Proc. Natl. Int. Ed.*, 2013, **110**, 3248–3253.
20 J. de Wit, *J. Dairy Sci.*, 1990, **73**, 3602–3612.
21 J. Kinsella and D. Whitehead, *Adv. Food Nutr. Res.*, 1989, **33**, 343–438.
22 A. Donald, *Soft Matter*, 2008, **4**, 1147–1150.
23 R. Mezzenga and P. Fischer, *Rep. Prog. Phys.*, 2013, **76**, 046601.
24 J. Gummel, F. Cousin and F. Boué, *J. Am. Chem. Soc.*, 2007, **129**, 5806–5807.
25 M. Semenova, *Food Hydrocolloids*, 2007, **21**, 23–45.
26 M. Pouzot, T. Nicolai, R. Visschers and M. Weijers, *Food Hydrocolloids*, 2005, **19**, 231–238.
27 N. Schmidt and G. Wong, *Curr. Opin. Solid State Mater. Sci.*, 2013, **17**, 151–163.
28 J. C. Dawson, J. A. Legg and L. M. Machesky, *Trends Cell Biol.*, 2006, **16**, 493–498.
29 M. Dubois, V. Lizunov, A. Meister, T. Gulik-Krzywicki, J. M. Verbavatz, E. Perez, J. Zimmerberg and T. Zemb, *Proc. Natl. Acad. Sci. U. S. A.*, 2004, **101**, 15082–15087.
30 J. Yoon, S. Cai, Z. Suo and R. C. Hayward, *Soft Matter*, 2010, **6**, 6004–6012.
31 M. Chekchaki and V. Lazarus, *Transp. Porous Media*, 2013, **100**, 143–157.
32 J. Skotheim and L. Mahadevan, *Proc. R. Soc. London, Ser. A*, 2004, **460**, 1995–2020.
33 R. Huang and S. H. Im, *Phys. Rev. E: Stat., Nonlinear, Soft Matter Phys.*, 2006, **74**, 026214.